

OCTOBER 1979

LRP 157/79

AN ALGORITHM TO COMPUTE THE VACUUM
CONTRIBUTION TO THE IDEAL MHD δW IN
AN AXISYMMETRIC CONFIGURATION

F. Troyon, L.C. Bernard, R. Gruber

AN ALGORITHM TO COMPUTE THE VACUUM CONTRIBUTION
TO THE IDEAL MHD δW IN AN AXISYMMETRIC CONFIGURATION

F. Troyon, L.C. Bernard, R. Gruber

Centre de Recherches en Physique des Plasmas
Association Euratom - Confédération Suisse
Ecole Polytechnique Fédérale de Lausanne
CH-1007 Lausanne / Switzerland

Abstract

In magnetohydrodynamic spectral codes, the change in the vacuum potential energy contained between the plasma surface and the conducting shell must be expressed in terms of the deformation of the plasma surface. For the case of a toroidal axisymmetric configuration a numerical scheme based on a Green's function formulation of the vacuum problem is presented. The results of test runs demonstrate that the method works well when the shell is arbitrarily close to the plasma surface.

1. Introduction

In the numerical computation of the ideal MHD spectrum of toroidal axisymmetric plasma configurations, the contribution of the vacuum potential energy in terms of the displacement at the plasma surface can be computed, either by a direct solution of a Laplace equation in the vacuum region {1} or by a Green's function technique which requires only a solution of coupled integral equations on the boundaries {2}. This last technique looks very attractive but its implementation has presented difficulties whenever the distance between the plasma and the boundary is of the order of or smaller than the discretization length on the surfaces.

The object of this paper is to describe a method which works equally well for any distance between the plasma and the shell. As the shell is progressively brought closer to the plasma, we have verified that the contribution of the vacuum becomes infinite as it should, leading to the correct rigid boundary condition in the limit of the shell tight against the plasma. This method has been implemented in the ERATO {3} and PEST stability codes {4}.

2. The Vacuum Potential Energy

We consider an axisymmetric toroidal plasma surrounded by a vacuum region, itself limited by an infinitely conducting shell (Fig. 1). The vacuum potential energy δW_v is given by

$$\delta W_v = \frac{1}{2} \int_V d\tau (\delta B^2), \quad (1)$$

where δB is the perturbed magnetic field, which satisfies the equation

$$\begin{aligned} \underline{\nabla} \times \underline{\delta B} &= 0 \\ \underline{\nabla} \cdot \underline{\delta B} &= 0 \end{aligned} \quad (2)$$

with the boundary conditions

$$\underline{v} \cdot \underline{\delta B} = 0 \quad \text{on the shell}(s) \quad (3)$$

$$\underline{v} \cdot \underline{\delta B} \quad \text{known on the plasma in terms of the normal}$$

displacement. The normal vector \underline{v} always points towards the vacuum region.

Introducing the scalar potential ϕ , such that

$$\underline{\delta B} = \underline{\nabla} \phi, \quad (4)$$

the potential energy can be reexpressed as an integral over the plasma surface (p) only

$$\delta W = \frac{1}{2} \int_p ds \phi \left(\frac{d\phi}{dv} \right) \quad (5)$$

where ϕ satisfies the equation

$$\underline{\Delta} \phi = 0 \quad (6)$$

and

$$d\phi/dv = 0 \quad (7)$$

on the shell.

The problem is then to evaluate δW in terms of $d\phi/dv$ on the plasma surface. This is done by solving equ. (6) for $\phi(\underline{x})$ with the boundary condition (7) and substituting into equ. (5).

3. Transformation into an Integral Equation

The scalar potential $\phi(\underline{x})$, solution of equ. 6, can be written as

$$\begin{aligned} \phi(\underline{x}) = & \frac{1}{2\pi} \int_p \left[\phi(\underline{x}') \frac{\partial G(\underline{x}, \underline{x}')}{\partial v'} - G(\underline{x}, \underline{x}') \frac{\partial \phi(\underline{x}')}{\partial v'} \right] ds' \\ & - \frac{1}{2\pi} \int_s \phi(\underline{x}') \frac{\partial G(\underline{x}, \underline{x}')}{\partial v'} ds' \end{aligned} \quad (8)$$

with

$$G(\underline{x}, \underline{x}') = \frac{1}{|\underline{x} - \underline{x}'|}, \quad (9)$$

where \underline{x}' is the integration variable and \underline{x} is a point in the vacuum region.

By letting successively the value of \underline{x} in equ. (8) approach a point \underline{x}_p on the plasma surface and \underline{x}_s on the shell, we obtain a system of 2 integral equations for $\phi_p(\underline{x}_p)$ and $\phi_s(\underline{x}_s)$ in terms of the known $\frac{\partial \phi}{\partial \nu}|_p$ on the plasma surface (5). The integrals are discontinuous functions of \underline{x} as \underline{x} approaches the boundary. To avoid these singularities we add and subtract integrals which have the same discontinuities:

$$\int_p ds' \frac{\partial G(\underline{x}, \underline{x}')}{\partial \nu'} = \begin{cases} 0 & \text{if } \underline{x} \text{ on the shell} \\ -2\pi & \text{if } \underline{x} \text{ on the plasma} \end{cases} \quad (10)$$

$$\int_s ds' \frac{\partial G(\underline{x}, \underline{x}')}{\partial \nu'} = \begin{cases} -2\pi & \text{if } \underline{x} \text{ on the shell} \\ -4\pi & \text{if } \underline{x} \text{ on the plasma} \end{cases}$$

This leads to the integral equations for ϕ_p and ϕ_s :

$$2\phi_p(\underline{x}_p) - 2\phi_s(\underline{x}_s) = \frac{1}{2\pi} \int_p \left[\phi_p(\underline{x}'_p) - \phi_p(\underline{x}_p) \right] \frac{\partial G(\underline{x}_p, \underline{x}'_p)}{\partial \nu'} ds' - \frac{1}{2\pi} \int_s \left[\phi_s(\underline{x}'_s) - \phi_s(\underline{x}_s) \right] \frac{\partial G(\underline{x}_p, \underline{x}'_s)}{\partial \nu'} ds' - \frac{1}{2\pi} \int_p G(\underline{x}_p, \underline{x}'_p) \frac{\partial \phi(\underline{x}'_p)}{\partial \nu'} ds' \quad (11)$$

$$0 = \frac{1}{2\pi} \int_p \left[\phi_p(\underline{x}'_p) - \phi_p(\underline{x}_p) \right] \frac{\partial G(\underline{x}_s, \underline{x}'_p)}{\partial \nu'} ds' - \frac{1}{2\pi} \int_s \left[\phi_s(\underline{x}'_s) - \phi_s(\underline{x}_s) \right] \frac{\partial G(\underline{x}_s, \underline{x}'_s)}{\partial \nu'} ds' - \frac{1}{2\pi} \int_s G(\underline{x}_s, \underline{x}'_p) \frac{\partial \phi(\underline{x}'_p)}{\partial \nu'} ds' \quad (12)$$

The integrals containing $\frac{\partial G}{\partial v}$ are now all regular. In the limit where the shell is tight against the plasma surface $\phi_s(\underline{x}) = \phi_p(\underline{x})$ all the terms of eq. 11 and 12 vanish except the source term leading to

$$\frac{\partial \phi_p(\underline{x})}{\partial v} = 0 \quad (13)$$

which states that the normal displacement of the plasma surface vanishes. This represents the correct boundary condition. This means that we have found a method which fulfills this limit automatically.

4. Fourier Decomposition

Let us introduce the polar coordinate system ρ, θ, φ (fig 1) in which:

$$\begin{aligned} \frac{\partial}{\partial v} &= \frac{1}{\ell} \frac{dz}{d\theta} \frac{\partial}{\partial r} - \frac{dr}{d\theta} \frac{\partial}{\partial z} \\ \ell &= \sqrt{\left(\frac{dr}{d\theta}\right)^2 + \left(\frac{dz}{d\theta}\right)^2} \\ ds &= \ell r d\varphi d\theta \end{aligned} \quad (14)$$

$$r = R + \rho \cos \theta$$

$$z = \rho \sin \theta$$

$$|\underline{x} - \underline{x}'| = \left[(r - r')^2 + (z - z')^2 + 4rr' \sin^2 \varphi / 2 \right]^{1/2} .$$

The source term $\frac{\partial \phi_p}{\partial v}$ and the potentials ϕ_p and ϕ_s can be Fourier analyzed in φ . Considering only one component we write

$$\frac{\partial \phi_p}{\partial v} = \frac{1}{\ell_p r_p} N(\theta_p) e^{in\varphi}, \quad (15)$$

$$\phi_{p,s}(\rho, \theta, \varphi) = \phi_{p,s}(\theta) e^{in\varphi},$$

where the integer n is the usual toroidal wave number. This treatment is strictly valid for $n \neq 0$ only. For $n = 0$ other terms {6} have to be added which do not change the essential features of the problem. These additional terms do not contribute in the case, important for the applications, when the equilibrium has the up-down symmetry.

Introducing the notations

$$G_{uv'}^n(\theta, \theta') \equiv \int_0^{2\pi} \frac{e^{in\varphi}}{|\underline{x}_u - \underline{x}_{v'}|} d\varphi \quad (16)$$

and

$$\underline{v}' \cdot \underline{\nabla}' G_{uv'}^n \equiv \frac{dz'}{d\theta'} \left(\frac{\partial G_{uv'}^n}{\partial r'} \right)_{z'} - \frac{dr'}{d\theta'} \left(\frac{\partial G_{uv'}^n}{\partial z'} \right)_{r'} \quad (17)$$

$$\begin{aligned} 2\phi_p(\theta) - 2\phi_s(\theta) &= \frac{1}{2\pi} \int_0^{2\pi} d\theta' r' \left[\underline{v}' \cdot \underline{\nabla}' G_{pp'}^n \phi_p(\theta') - \underline{v}' \cdot \underline{\nabla}' G_{pp'}^0 \phi_p(\theta) \right] - \\ &- \frac{1}{2\pi} \int_0^{2\pi} d\theta' G_{pp'}^n N(\theta') - \frac{1}{2\pi} \int_0^{2\pi} d\theta' r' \left[\underline{v}' \cdot \underline{\nabla}' G_{ps'}^n \phi_s(\theta') - \underline{v}' \cdot \underline{\nabla}' G_{ps'}^0 \phi_s(\theta) \right] \end{aligned} \quad (18)$$

$$\begin{aligned} 0 &= \frac{1}{2\pi} \int_0^{2\pi} d\theta' r' \left[\underline{v}' \cdot \underline{\nabla}' G_{sp'}^n \phi_p(\theta') - \underline{v}' \cdot \underline{\nabla}' G_{sp'}^0 \phi_p(\theta) \right] - \\ &- \frac{1}{2\pi} \int_0^{2\pi} d\theta' G_{pp'}^n N(\theta') - \frac{1}{2\pi} \int_0^{2\pi} d\theta' r' \left[\underline{v}' \cdot \underline{\nabla}' G_{ss'}^n \phi_s(\theta') - \underline{v}' \cdot \underline{\nabla}' G_{ss'}^0 \phi_s(\theta) \right] \end{aligned} \quad (19)$$

The solution of equations (18) and (19) will have the form

$$\phi_p(\theta) = \int_p Q(\theta, \theta') N(\theta') d\theta'. \quad (20)$$

Substituting into equation (5) will then give us δW in terms of the source $N(\theta)$:

$$\delta W = \frac{1}{2} \iint_p d\theta d\theta' Q(\theta, \theta') N(\theta') N(\theta) \quad (21)$$

We now tackle the problem of finding a numerical algorithm to solve eqs. (18) and (19).

5. Singularities of the Green's Function

Defining the modified elliptic integral K_n to be

$$K_n(\eta) = (-1)^n \int_0^{\pi/2} \frac{\cos(2n\alpha) d\alpha}{[\cos^2 \alpha + \eta \sin^2 \alpha]^{\frac{1}{2}}} \quad (22)$$

where

$$\eta = \frac{(r'_v - r_u)^2 + (z'_v - z_u)^2}{(r'_v + r_u)^2 + (z'_v - z_u)^2} \quad (23)$$

the integral (16) becomes

$$G_{uv'}^n = \frac{4K_n(\eta)}{[(r'_v + r_u)^2 + (z'_v - z_u)^2]^{\frac{1}{2}}} \quad (24)$$

The integral K_n has a logarithmic singularity at $\eta = 0$:

$$K_n(\eta) = -\frac{\ln \eta}{2} + \dots \quad (25)$$

This singularity is removed in all the terms, except in the source term

$$S_{uv'}(\theta) = \frac{1}{2\pi} \int_0^{2\pi} d\theta' G_{uv'}^n N(\theta') \quad (26)$$

which can be rewritten as

$$S_{uv'} = S_{reg} + S_{anal}$$

where

$$\begin{aligned} S_{reg} &= \frac{1}{2\pi} \int_0^{2\pi} d\theta' \left\{ G_{uv'}^n N(\theta') + \frac{1}{r} \ln[\Delta^2 + (\theta - \theta')^2] N(\theta) \right\} \\ S_{anal} &= -\frac{N(\theta)}{2\pi r} \int_0^{2\pi} d\theta' \ln[\Delta^2 + (\theta - \theta')^2], \\ \Delta^2 &= \frac{(\rho - \rho')^2}{\rho\rho'} \end{aligned} \quad (27)$$

S_{reg} is now a regular integral which can be integrated numerically, while S_{anal} contains the singularity and will be integrated analytically.

6. Discretisation of the Integral Equations

We divide the vacuum region in N_θ non-equidistant intervals such that $\theta_1 = 0$ and $\theta_{N_\theta+1} = 2\pi$. In order to solve the system of coupled equations (18,19), we expand $N(\theta)$, $\phi_p(\theta)$ and $\phi_s(\theta)$ in terms of finite elements $f_{i+\frac{1}{2}}$, piecewise constant over the interval (θ_i, θ_{i+1}) :

$$\begin{aligned} N(\theta) &= \sum_{i=0}^N a^{i+\frac{1}{2}} f_{i+\frac{1}{2}} \\ \phi_p(\theta) &= \sum_{i=0}^N b^{i+\frac{1}{2}} f_{i+\frac{1}{2}} \\ \phi_s(\theta) &= \sum_{i=0}^N c^{i+\frac{1}{2}} f_{i+\frac{1}{2}} \end{aligned} \quad , \quad (28)$$

integrate over θ and end up with a set of coupled matrix equations

$$\begin{aligned} \underline{2b} - \underline{2c} &= \underline{A} \cdot \underline{b} - \underline{B} \underline{a} - \underline{C} \underline{c} \\ 0 &= \underline{D} \underline{b} - \underline{E} \underline{a} - \underline{F} \underline{c} \end{aligned} \quad . \quad (29)$$

The matrix elements are

$$\begin{aligned} {}_{pp'}^{ij} &= \frac{1}{2\pi\Delta\theta_{i+\frac{1}{2}}} \int_{\theta_i}^{\theta_{i+1}} d\theta f_{i+\frac{1}{2}} \left\{ \int_{\theta_j}^{\theta_{j+1}} d\theta' f_{j+\frac{1}{2}} r'_{\underline{v}'} \cdot \underline{\nabla}' G_{pp'}^n - f_{i+\frac{1}{2}} \delta_{ij} \int_0^{2\pi} d\theta' r'_{\underline{v}'} \cdot \underline{\nabla}' G_{pp'}^o \right\} \\ {}_{pp'}^{ij} &= \frac{1}{2\pi\Delta\theta_{i+\frac{1}{2}}} \int_{\theta_i}^{\theta_{i+1}} d\theta f_{i+\frac{1}{2}} \left\{ \int_{\theta_j}^{\theta_{j+1}} d\theta' f_{j+\frac{1}{2}} \left(G_{pp}^n + \frac{\delta_{ij}}{r} \ln[\Delta^2 + (\theta - \theta')^2] \right) - f_{i+\frac{1}{2}} \frac{\delta_{ij}}{r} \int_{\theta_i}^{\theta_{i+1}} \ln \Delta^2 + (\theta - \theta')^2 d\theta' \right\} \\ {}_{ps'}^{ij} &= \frac{1}{2\pi\Delta\theta_{i+\frac{1}{2}}} \int_{\theta_i}^{\theta_{i+1}} d\theta f_{i+\frac{1}{2}} \left\{ \int_{\theta_j}^{\theta_{j+1}} d\theta' f_{j+\frac{1}{2}} r'_{\underline{v}'} \cdot \underline{\nabla}' G_{ps'}^n - f_{i+\frac{1}{2}} \delta_{ij} \int_0^{2\pi} d\theta' r'_{\underline{v}'} \cdot \underline{\nabla}' G_{ps'}^o \right\} \\ {}_{sp'}^{ij} &= \frac{1}{2\pi\Delta\theta_{i+\frac{1}{2}}} \int_{\theta_i}^{\theta_{i+1}} d\theta f_{i+\frac{1}{2}} \left\{ \int_{\theta_j}^{\theta_{j+1}} d\theta' f_{j+\frac{1}{2}} r'_{\underline{v}'} \cdot \underline{\nabla}' G_{sp'}^n - f_{i+\frac{1}{2}} \delta_{ij} \int_0^{2\pi} r'_{\underline{v}'} \cdot \underline{\nabla}' G_{sp'}^o \right\} \end{aligned} \quad ($$

$$E_{sp'}^{ij} = \frac{1}{2\pi\Delta\theta_{i+\frac{1}{2}}} \int_{\theta_i}^{\theta_{i+1}} d\theta f_{i+\frac{1}{2}} \left\{ \int_{\theta_j}^{\theta_{j+1}} d\theta' f_{j+\frac{1}{2}} \left(G_{sp'}^n + \frac{\delta_{ij}}{r} \ln[\Delta^2 + (\theta - \theta')^2] \right) - f_{i+\frac{1}{2}} \frac{\delta_{ij}}{r} \int_{\theta_i}^{\theta_{i+1}} \ln[\Delta^2 + (\theta - \theta')^2] \right\} \quad (3)$$

$$F_{ss'}^{ij} = \frac{1}{2\pi\Delta\theta_{i+\frac{1}{2}}} \int_{\theta_i}^{\theta_{i+1}} d\theta f_{i+\frac{1}{2}} \left\{ \int_{\theta_j}^{\theta_{j+1}} d\theta' f_{j+\frac{1}{2}} r' \underline{v}' \cdot \underline{\nabla}' G_{ss'}^n - f_{i+\frac{1}{2}} \delta_{ij} \int_0^{2\pi} r' \underline{v}' \cdot \underline{\nabla}' G_{ss'}^0 \right\}$$

Eliminating \underline{c} from eq. (29) we obtain

$$\underline{b} = \underline{Q} \cdot \underline{a}$$

$$\underline{Q} = \left[\underline{A} - 2\underline{I} - (\underline{C} - 2\underline{I}) \underline{F}^{-1} \underline{D} \right]^{-1} \left[\underline{B} - (\underline{C} - 2\underline{I}) \underline{F}^{-1} \underline{E} \right]. \quad (31)$$

Whenever the wall is close to the plasma ($\|\underline{\epsilon}\| \ll \|\underline{A}\|$):

$$\begin{aligned} \underline{C} &\approx \underline{A} - \underline{\epsilon} \\ \underline{D} &\approx \underline{A} + \underline{\epsilon} \\ \underline{F} &\approx \underline{A} \\ \underline{E} &\approx \underline{B} \end{aligned}, \quad (32)$$

\underline{Q} becomes $\underline{Q} \approx \underline{\epsilon}^{-1} \underline{B}$. (33)

Note that for a wall tight on the plasma surface all subdeterminants of \underline{Q} are ∞ . This implies that $\underline{a} \rightarrow \underline{0}$ which corresponds to the exact condition $N(\theta) = 0$. Also note, that the way that we calculate the matrices enables us to pick up this singular behaviour of \underline{Q} and, therefore, it is possible with this method to have the wall arbitrarily close to the plasma as we shall demonstrate (Fig. 3).

7. Numerical Integrations

The regular integrals in (30) are performed by means of a 4 point integration formula

$$\int_{x=-\frac{h}{2}}^{\frac{h}{2}} \int_{y=-\frac{h'}{2}}^{\frac{h'}{2}} f(x,y) dx dy = hh' \left[f\left(-\frac{h}{\sqrt{6}}, 0\right) + f\left(0, -\frac{h'}{\sqrt{6}}\right) + f\left(\frac{h}{\sqrt{6}}, 0\right) + f\left(0, \frac{h'}{\sqrt{6}}\right) \right] \quad (34)$$

It is an integration rule in $O(h^4)$ which does not use values of the function on the diagonal (figure 2) on which we would meet numerical problems due to the cancellation of the singularities.

In the code, the singular part of S_{anal} (equ. 27) is calculated analytically, i.e. :

$$S_{\text{anal}} = -\frac{1}{2\pi} \sum_i a^{i+\frac{1}{2}} \int_{\theta_i}^{\theta_{i+1}} d\theta \frac{f_{i+\frac{1}{2}}}{r_{i+\frac{1}{2}}} \int_{\theta_i}^{\theta_{i+1}} d\theta' 2 \ln \left[\Delta^2 + (\theta_{i+1} - \theta_i)^2 \right] \quad (35)$$

Note that for the matrix B (equ. 30), ρ and ρ' are on the plasma surface and at $\theta' = \theta$, $\rho' = \rho$ (i.e. $\Delta = 0$) there is a logarithmic singularity (equ. 35).

In the integral E, however, there is no singularity but for a wall near the plasma surface (when Δ is smaller than the mesh size) an apparent logarithmic singularity is built up numerically. We avoid the problem by treating these integrals, B and E, analytically.

$$\begin{aligned} \int_{\theta_i}^{\theta_{i+1}} d\theta \int_{\theta_i}^{\theta_{i+1}} d\theta' \ln [\Delta^2 + (\theta - \theta')^2] &= -3 (\theta_{i+1} - \theta_i)^2 + \\ &+ 4\Delta (\theta_{i+1} - \theta_i) \operatorname{Atg} \frac{\theta_{i+1} - \theta_i}{\Delta} + \Delta^2 \ln \Delta^2 + \\ &+ [-\Delta^2 + (\theta_{i+1} - \theta_i)^2] \ln [\Delta^2 + (\theta_{i+1} - \theta_i)^2] \quad (36) \end{aligned}$$

Here Δ^2 is considered to be constant in the interval $\theta_i \leq \theta < \theta_{i+1}$, i.e. $\Delta^2 = 0$ for the matrix B (the value of the integral is then $-(\theta_{i+1} - \theta_i) \{3 - \ln(\theta_{i+1} - \theta_i)^2\}$) and $\Delta^2 = (\rho_p - \rho_c)^2 / \rho_p \rho_c$ at $\theta = (\theta_{i+1} + \theta_i) / 2$ for the matrix E).

8. Results of Test Runs

The method described has been implemented in ERATO, an ideal MHD spectral code which computes the eigenmodes of a toroidal axisymmetric plasma configuration. We choose as a test case to run the Solovèv equilibrium {7}, which we already have run with the so-called "old" method. This old method, described in {5}, uses the same starting point, namely the integral equation (8); the singular terms in the integrals are subtracted off and integrated separately. The identities (10) are then only approximately satisfied.

The results of the comparison runs are shown in figure 3. The configuration itself is shown in figure 1. The plasma has an elongation of 2, an aspect ratio of 3 and the eigenvalue λ plotted represents the square of the growth rate of the most unstable $n=1$ mode normalized to the Alfvén transit time across the main radius of the plasma. The important parameter is R_{ext} which fixes the distance between the conducting shell and the plasma surface (figure 1). When R_{ext} is too large, the shell crosses the main axis of the torus, in which case we cut off the unphysical part of the shell and complete the shell with a wire on the main axis. In our test the effect of this wire is so small that the case $R_{ext} = \infty$ can be considered as identical to the case without a shell. When $R_{ext} = 1$, the shell is tight against the plasma and prevents any surface displacement. This is the rigid boundary limit which can be directly computed by omitting the vacuum contribution and forcing the normal component of the displacement to vanish at the surface. The result of this calculation appears in figure 3 as a circle at $R_{ext} = 1$. The variation of the eigenvalue λ as a function of R_{ext} is shown in figure 3. The

old and new methods agree at large values of R_{ext} , but the limit $R_{\text{ext}} = 1$ is only reproduced by the new method. The value of R_{ext} below which the old method becomes incorrect depends on the size of the mesh used to solve the integral equations. The calculation in figure 3 has been done with 56 intervals. For a given R_{ext} , the two methods give the same result in the limit $N_{\theta} \rightarrow \infty$; but in ERATO the computing time grows as N_{θ}^3 and the range of interest of R_{ext} turns out to be of the order of 1.1 to 2. It is impossible with present computers to have a sufficient resolution to use the old method.

The described Green's function method is asymmetric in its treatment of the two variables θ, θ' and it does not lead to an explicitly symmetric kernel $Q(\theta, \theta')$. Because of the discretization errors the matrix Q_{ij} is not symmetric. This lack of symmetry can be measured by the quantity

$$\sigma^2 = \frac{\sum_{i,j=1}^{N_{\theta}} (Q_{ij} - Q_{ji})^2}{\sum_{i,j=1}^{N_{\theta}} Q_{ij}^2} \quad (37)$$

Figure 4 shows σ^2 as a function of N_{θ}^{-4} for $R_{\text{ext}} = 2$. The fact that the matrix becomes indeed symmetric in the limit $N_{\theta} \rightarrow \infty$ is a verification of the correctness of the method and of the coding. Practically, in ERATO, we have to have Q_{ij} symmetric and we do this by introducing $\bar{Q}_{ij} = (Q_{ij} + Q_{ji})/2$. The error is $O(N_{\theta}^{-4})$ and is thus of higher order than the error in the elements of the matrix themselves.

9. Conclusions

We have presented a Green's function method to compute the change in the vacuum potential energy of a toroidal axisymmetric region which surrounds a toroidal plasma column, due to the displacement of the plasma surface and

which works for any thickness of the vacuum region. This method is now implemented in the standard version of ERATO which is used by many groups to study β limits in Tokamaks.

This work has been supported in part by the Swiss National Science Foundation.

References:

- (1) D. Berger, R. Gruber, F. Troyon, Computer Phys. Commun. 11, 313 (1976)
- (2) B.M. Marder, Phys. Fluids 17, 634 (1974)
- (3) D. Berger, R. Gruber, F. Troyon, Proc. 2nd Europ. Conf. on Comp. Phys. (D. Biskamp ed.) Garching (1976) paper C3
- (4) R.C. Grimm, J.M. Greene, J.L. Johnson, in "Method of Computational Physics" (Academic Press, N.Y.) Vol. 16, Chapter 4 (1976)
- (5) L.C. Bernard, D. Berger, R. Gruber, F. Troyon, ZAMP 28, 353 (1977)
- (6) R. Lüst and R. Martensen, Z. Naturforschung 15a, 706 (1960)
- (7) L.S. Solovèv, JETP 26, (1968), 400

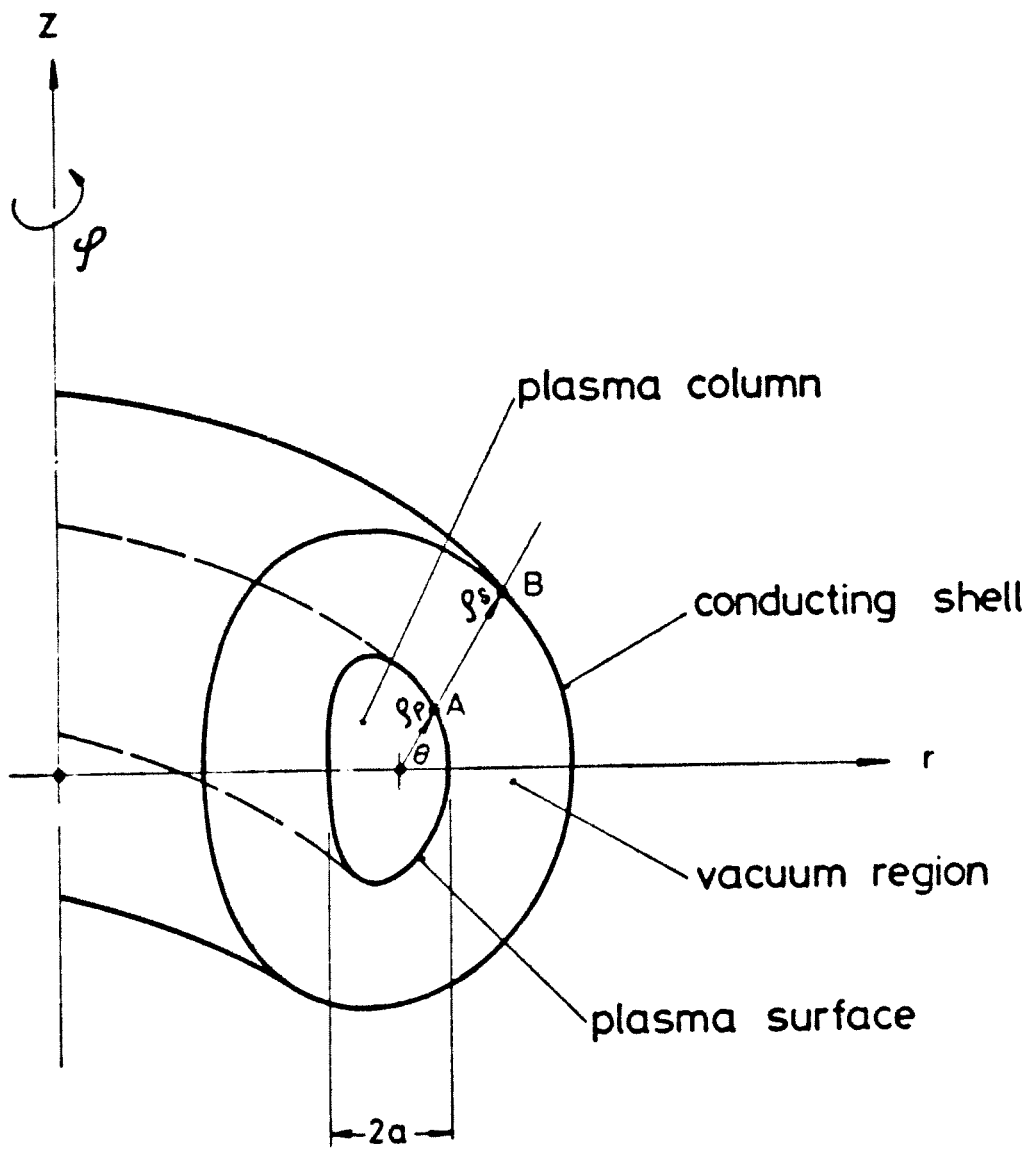
Figure Captions

Fig. 1: The configuration and the coordinate systems. The conducting shell surrounds the plasma. $AB = (R_{\text{ext}} - 1) a$.

Fig. 2: The positions of the 4 points in a mesh cell used in the numerical integration (34).

Fig. 3: The eigenvalue λ as a function of the distance between the shell and the plasma for $N_{\theta} = 56$. The Solovèv equilibrium is characterized by an aspect ratio of 3, an elongation of 2, $q_{\text{axis}} = 0.666$ and $n = 1$. The abscissa x is proportional to $(1 - R_{\text{ext}}^{-2})$. The solid curve is obtained with the new method while the dotted curve is obtained with the old method {5}. The circle at $R_{\text{ext}} = 1$ is the exact rigid boundary value.

Fig. 4: The asymmetry of the Q matrix as a function of the number of elements N_{θ} for $R_{\text{ext}} = 2$. The abscissa is proportional to N_{θ}^{-4} .



$$AB = (R_{ext} - 1) a$$

Figure 1.

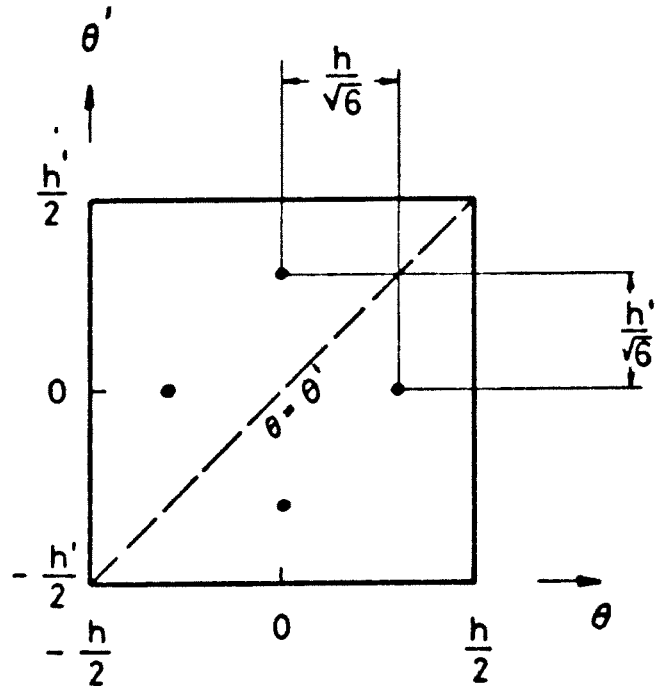


Figure 2.

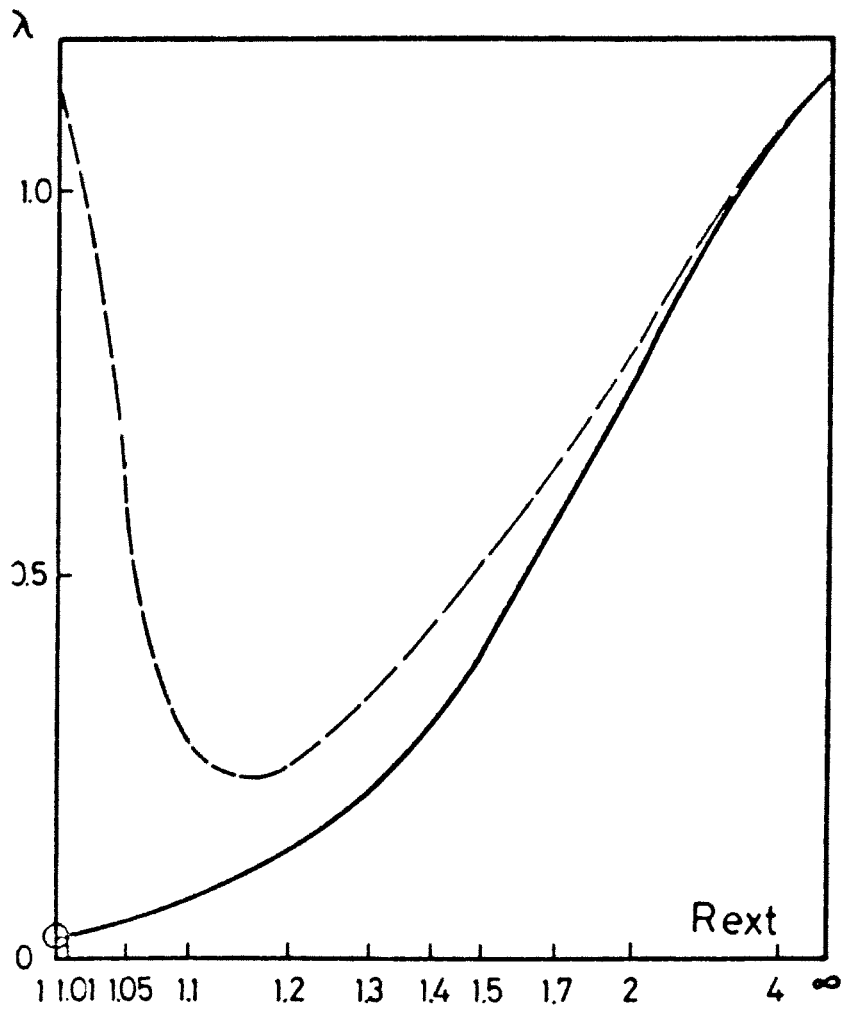


Figure 3.

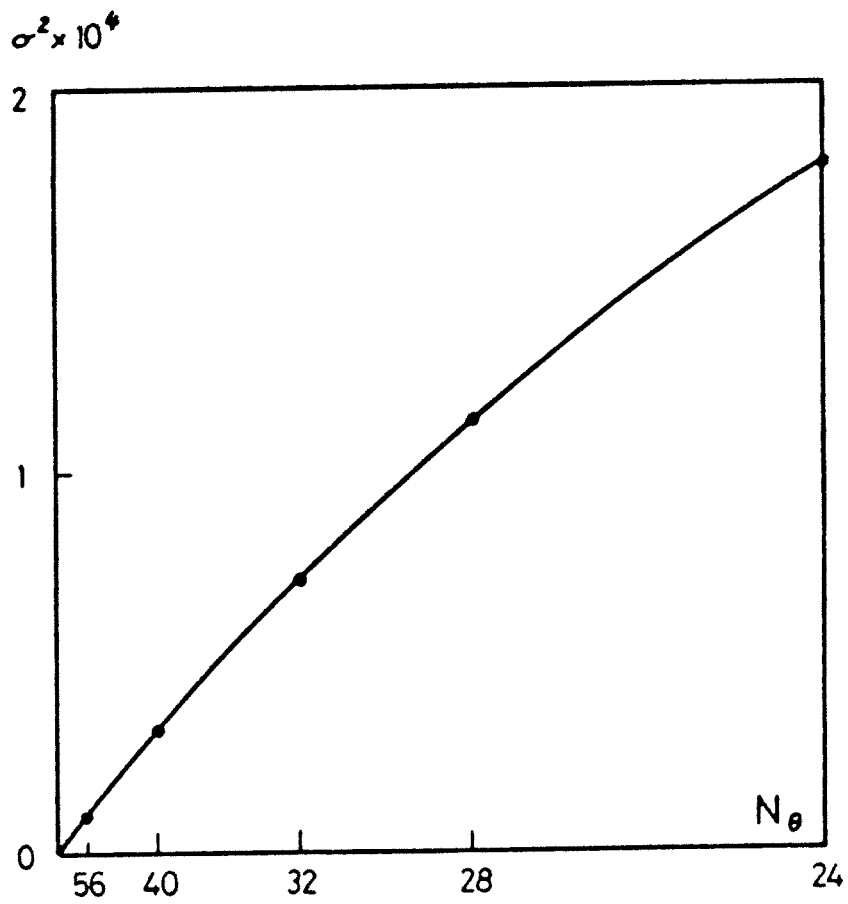


Figure 4.